Inorganic Chemistry

Article

Cite This: Inorg. Chem. XXXX, XXX, XXX-XXX

pubs.acs.org/IC

Synthesis, Characterization, and Properties of Iron(II) Spin-Crossover Molecular Photoswitches Functioning at Room Temperature

Max Mörtel,[‡] Alexander Witt,[‡] Frank W. Heinemann, Sebastian Bochmann, Julien Bachmann, and Marat M. Khusniyarov*

Department of Chemistry and Pharmacy, Friedrich-Alexander University Erlangen-Nürnberg, Egerlandstrasse 1, 91058 Erlangen, Germany

Supporting Information

ABSTRACT: Spin-crossover molecular switches $[Fe^{II}(H_2B(pz)_2)_2L]$ (**L** = novel phenanthroline-based ligands featuring photochromic diarylethene units; pz = 1-pyrazolyl) were synthesized and thoroughly characterized by variable-temperature X-ray crystallography, Mössbauer spectroscopy, and magnetic measurements. The effect of substituents introduced into the phenanthroline backbone (**L2**) and into the photochromic diarylethene unit (**L3**) on photophysical properties of metal-free ligands and spin-crossover iron(II) complexes **2** and **3**, respectively, were investigated in detail. Both ligands and complexes could be switched with light in solution at room temperature. The photocyclization of **2** was accompanied by a high-spin to low-spin photoconversion determined at 19%. The closed-ring isomers of **L3** and **3** reveal the lifetimes in the range of minutes, whereas those of **L2** and **2** are thermally stable for days in solutions at room temperature. The reversibility of the photoswitching can be improved by avoiding the photostationary states. Prospective introduction of anchoring groups to the phenanthroline backbone might allow the construction of chemisorbed self-assembled monolayers of spin-crossover species switchable with light at room temperature.

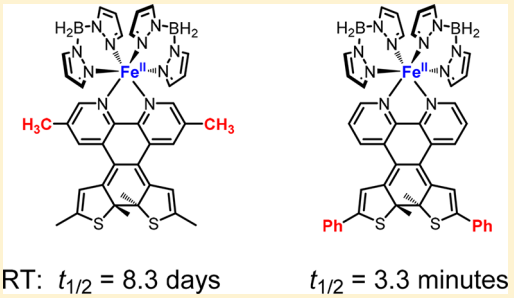

INTRODUCTION

Spin-crossover (SCO) metal complexes represent a highly promising class of molecular switches, whose magnetic, conductive, and other physical properties can be reversibly altered by different physical stimuli including a change in temperature, applied pressure, light irradiation, and applied electric and magnetic fields.[1,2] Among SCO complexes, six-coordinate iron(II) species are the most common representatives that offer a brilliant opportunity to switch reversibly between diamagnetic low-spin (LS) and paramagnetic high-spin (HS) electronic states. The ability for reversible switching of diverse physical properties by an external stimulus of choice renders SCO complexes highly promising candidates for many future applications including molecular sensors,[3] luminescent, plasmonic,[4] and display devices,[5] ultrahigh-density memories,[6] and building blocks for molecular electronics and spintronics.[7,8]

The photoswitching of SCO species is very attractive because of the extremely fast switching (sub-picoseconds)[9] and low power dissipation. Thus, photoswitching of SCO thin films and monolayers via a light-induced excited spin-state trapping (LIESST) effect was achieved recently.[10−15] However, very low temperatures (usually below 50 K) are strictly mandatory here, because the photoinduced state in the LIESST effect is thermally unstable and relaxes to the ground state within nanoseconds at room temperature (RT).[16−19] Thus, the photoswitching of immobilized SCO molecular complexes at RT, which is an important goal in photomagnetic materials, has never been achieved. Alternative concepts for the photoswitching at RT are needed.[20]

Targeting the switching of magnetic properties at RT,[21,22] very recently, we synthesized a unique iron(II) SCO molecular switch **1** featuring a photoactive diarylethene-based ligand **L1** (Scheme 1).[23] Remarkably, **1** was reversibly switched between HS and LS states by irradiation with light at RT.[23,24] The photoswitching in **1** is fundamentally different from the previous examples, because it proceeds indirectly via the photoreaction at the photoisomerizable ligand, that is, a ligand-driven light-induced spin change (LD-LISC) effect.[25,26] Here, the photocyclization of the ligand triggers an SCO at the coordinated metal ion *remotely*. Although such ligand-driven photoswitching was suggested and attempted with other systems before,[25,27−31] only recently our group[23,24] and the group of Herges[32] achieved efficient and reversible photoswitching of iron(II) and nickel(II) molecular systems at RT, respectively. Importantly, such indirect photoswitching proceeds at the single-molecule level, and the photoisomers might be stable for years at RT.[33]

Currently, we successfully switched **1** with light at RT both in solution and in the solid state.[23,24] However, a question appears, namely, is **1** a unique fine-tuned molecular switch, or is it a member of a novel class of advanced magnetic photoswitches? The present work provides the answer to this

Received: July 31, 2017

DOI: 10.1021/acs.inorgchem.7b01952
Inorg. Chem. XXXX, XXX, XXX−XXX

Scheme 1. Diarylethene-Based Ligands L1−L3 and Corresponding Iron(II) Spin-Crossover Complexes 1−3

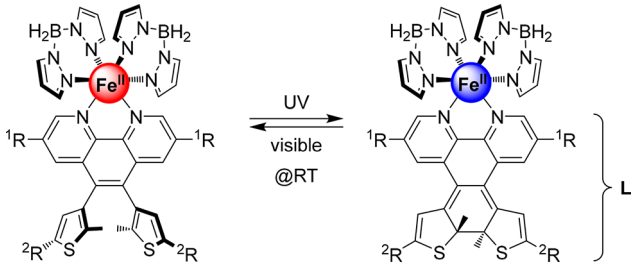

L1 / 1: ^{1}R = H, ^{2}R = Me

L2 / 2: ^{1}R = Me, ^{2}R = Me

L3 / 3: ^{1}R = H, ^{2}R = Ph

question. Here, we report on two novel derivatives of **1**. We successfully modified the parent diarylethene-based ligand **L1** by introducing methyl substituents into the phenanthroline backbone (**L2**) and phenyl groups into the photoactive diarylethene unit (**L3**, Scheme 1). The corresponding iron(II) SCO molecular switches **2** and **3** were subsequently synthesized. The physical, spectroscopic, and photophysical properties of novel ligands and their iron(II) complexes were investigated in detail and compared with the properties of the parent **L1**/**1** system.

EXPERIMENTAL SECTION

Materials. All starting materials and solvents were utilized as received without further purification unless otherwise noted. Pure anhydrous solvents were collected from a solid-state solvent purification system (Glass Contour; Irvine, CA). 3,8-Dimethyl-1,10-phenanthroline,[34] (2,5-dimethylthiophen-3-yl)boronic acid,[35,36] bis(1-pyrazolyl)borohydride,[37] (2-methyl-5-phenylthiophen-3-yl)boronic acid,[38,39] and 5,6-dibromo-1,10-phenanthroline[40] were prepared according to literature methods with minor modifications.

Instrumentation. Elemental analyses were performed with an EURO EA analyzer from EuroVector. Magnetic susceptibility data on solid samples were collected with a Quantum Design MPMS 5XL SQUID magnetometer. The direct-current (dc) susceptibility data were collected in the temperature range of 2−300 K on powder samples restrained within a polycarbonate gel capsule in the applied magnetic field of 1 T at 1 K min^{-1} heating/cooling rate and 2 K intervals. ^{57}Fe Mossbauer spectra were recorded on a WissEl Mossbauer spectrometer (MRG-500) in constant-acceleration mode. ^{57}Co/Rh was used as the radiation source. The temperature of the samples was controlled by an MBBC-HE0106 Mossbauer He/N_2 cryostat within an accuracy of ±0.3 K. Isomer shifts were determined relative to α-iron at 298 K. The program *MFIT* was used for the quantitative analysis of spectra.[41] NMR spectra were recorded with JEOL ECX 400 MHz, JEOL ECP 400 MHz, and JEOL EX 270 MHz in rotating 5 mm o.d. tubes and processed with *Delta V4.0* software provided by JEOL Ltd. Electronic absorption spectra were recorded with Shimadzu UV 2450 and Shimadzu UV 3600 spectrophotometers. Powder X-ray diffraction was performed in the Bragg−Brentano geometry on a Bruker D8 Advance equipped with a Cu Kα source and LynxEye XE T detector.

Photochemisty. All solutions for photoexperiments were prepared under inert conditions and sealed in custom-made Quartz SUPRASIL cells (QS). An L.O.T.-Oriel Xe(OF) 150 W arc lamp equipped with appropriate filters was used as a light source. Water and bandpass (λ = 282 ± 5 nm) filters were used for cyclization with UV, while a set of water, heat absorbing (KG-5), and long-pass ($\lambda \geq 400$ nm) filters was used for cycloreversion with visible.

Synthesis. *5,6-Dibromo-3,8-dimethyl-1,10-phenanthroline.* Under vigorous stirring 3,8-dimethyl-1,10-phenanthroline (5.00 g, 24.0 mmol) was added to a 65% oleum (35 mL) at 0 °C to give a brown viscous mixture. The mixture was stirred at RT for 20 min to ensure that the reagent dissolved completely. After the reaction flask was protected from light, Br_2 (7.67 g, 48.0 mmol) was added dropwise at 0 °C, and the reaction mixture was stirred for 20 h at RT. The dark brown mixture was then carefully poured on ice, and the resulting brown suspension was neutralized (pH ≈ 7) with a 25% NaOH solution. The aqueous phase was extracted with CH_2Cl_2, while insoluble residue, which hindered phase separation, was filtered off. The organic extracts were dried over $MgSO_4$ and filtered, and after solvent removal a yellow crude product was dried in vacuo. Recrystallization from $CHCl_3$ rendered needle-shaped colorless crystals of 5,6-dibromo-3,8-dimethyl-1,10-phenanthroline. Yield: 4.64 g, 53%. Anal. Calcd for $C_{14}H_{10}Br_2N_2$: C 45.94, H 2.75, N 7.65; found: C 46.00, H 2.68, N 7.57%. High-resolution mass spectrometry (HRMS) (electrospray ionization (ESI+)): m/z calcd. for $[M + Na]^+$ 388.9083, found 388.9086; for $[M + K]^+$ 404.8822, found 404.8832. ^{1}H NMR (400 MHz, $CDCl_3$, 21.4 °C) δ: 8.98 (s, 2 H, C_{aryl}−H), 8.42 (s, 2 H, C_{aryl}−H), 2.63 (s, 6 H, CH_3) ppm. ^{13}C NMR (67.8 MHz, $CDCl_3$, 25.0 °C) δ: 152.3, 143.4, 136.4, 134.2, 127.8, 124.8 (C_{aryl}), 18.8 (CH_3) ppm.

5,6-Bis(2,5-dimethylthiophen-3-yl)-3,8-dimethyl-1,10-phenanthroline (L2). Under inert atmosphere, degassed water (13.8 g, 764 mmol) was added to a suspension of 5,6-dibromo-3,8-dimethyl-1,10-phenanthroline (2.00 g, 54.6 mmol), (2,5-dimethylthiophen-3-yl)-boronic acid (5.11 g, 32.8 mmol), K_3PO_4 (23.2 g, 109 mmol), and $[Pd(dppf)Cl_2]\cdot CH_2Cl_2$ (1.34 g, 16.4 mmol, dppf = 1,1′-bis-(diphenylphosphino)ferrocene) in dry degassed 1,4-dioxane (120 mL), and the reaction mixture was stirred for 3 d at 100 °C. After solvent removal and drying in vacuo, the remaining solids were suspended in CH_2Cl_2 and water. The aqueous phase was separated and further extracted with CH_2Cl_2. The combined organic extracts were dried over $MgSO_4$ and filtered, and the solvent was removed in vacuo to give a crude brown product. Purification was achieved by flash chromatography on SiO_2 with $CHCl_3$. Solvent removal and extensive drying in vacuo rendered **L2** containing residual $CHCl_3$. Yield: 2.10 g, 74%. Anal. Calcd for $C_{26}H_{24}N_2S_2\cdot(CHCl_3)_{0.65}$: C 63.23, H 4.91, N 5.53, S 12.67; found: C 63.41, H 5.04, N 4.95, S 11.90%. HRMS (ESI+): m/z calcd. for $[M + H]^+$ 429.1454, found 429.1443; for $[M + K]^+$ 467.1012, found 467.1000; for $[2M + Na]^+$ 879.2654, found 879.2636; for $[2M + K]^+$ 895.2393, found 895.2373. ^{1}H NMR (400 MHz, $CDCl_3$, 22.8 °C) δ (conformer-1): 9.023 (s, 2 H, $C(2,9)_{phen}$−H), 7.694 (dd, ^4J = 2.1 Hz, J = 0.9 Hz, 2 H, $C(4,7)_{phen}$−H), 6.317 (d, J = 1.0 Hz, 2 H, $C_{thiophene}$−H), 2.505 (s, 6 H, C_{phen}−CH_3), 2.376 (s, 6 H, $C_{thiophene}$−CH_3), 1.976 (s, 6 H, $C_{thiophene}$−CH_3) ppm; δ (conformer-2): 9.019 (s, 2 H, $C(2,9)_{phen}$−H), 7.751 (dd, ^4J = 2.1 Hz, J = 0.9 Hz, 2 H, $C(4,7)_{phen}$−H), 6.327 (d, J = 1.0 Hz, 2 H, $C_{thiophene}$−H), 2.511 (s, 6 H, C_{phen}−CH_3), 2.387 (s, 6 H, $C_{thiophene}$−CH_3), 1.930 (s, 6 H, $C_{thiophene}$−CH_3) ppm. ^{13}C NMR (100.6 MHz, $CDCl_3$, 25.6 °C) δ: 151.1 (C_t), 143.1 (C_q), 135.6 (C_q), 135.5 (C_q), 134.7 (C_t), 134.5 (C_t), 134.2 (C_q), 133.8 (C_q), 133.3 (C_q), 133.2 (C_q), 132.9 (C_q), 128.3 (C_t), 128.2 (C_q), 128.1 (C_q), 127.2 (C_t), 19.01 (CH_3), 15.25 (CH_3), 14.10 (CH_3) ppm. Crystallization from MeOH solution rendered colorless block-shaped crystals suitable for X-ray structure determination.

3,8-Dimethyl-5,6-bis(2-methyl-5-phenylthiophen-3-yl)-1,10-phenanthroline (L3). Under inert atmosphere, dry 1,4-dioxane (16 mL) was added to a suspension of (2-methyl-5-phenylthiophen-3-yl)-boronic acid (0.99 g, 4.54 mmol), 5,6-dibromo-1,10-penanthroline (516 mg, 1.53 mmol), $[Pd(PPh_3)_4]$ (353 mg, 0.31 mmol), and anhydrous sodium carbonate (971 mg, 9.2 mmol) in degassed water (16 mL). The reaction mixture was stirred vigorously for 3 d at 95 °C. After it cooled to RT the aqueous layer was separated and extracted several times with CH_2Cl_2. The combined organic phases were washed with water and brine, dried over $MgSO_4$ and filtered, and the solvent was removed in vacuo to give a crude sand brown solid. Purification

DOI: 10.1021/acs.inorgchem.7b01952
Inorg. Chem. XXXX, XXX, XXX−XXX

Scheme 2. Syntheses of Novel Diarylethene-Based Ligands L2 and L3

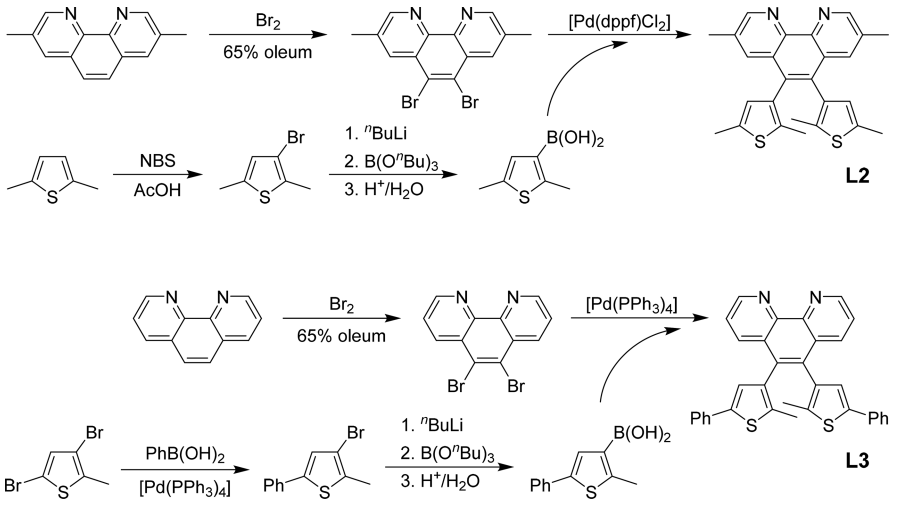

was achieved by washing with *n*-hexane followed by the flash column chromatography on SiO_2 with $CHCl_3$. Solvent removal and drying in vacuo yielded pure **L3** as an off-white powder. Yield: 0.55 g, 69%. Anal. Calcd (%) for $C_{34}H_{24}N_2S_2$: C 77.83, H 4.61, N 5.34, S 12.22; found: C 77.36, H 4.53, N 5.22, S 11.96. HRMS (ESI+): *m*/*z* calcd. for $[M + H]^+$ 525.1459, found 525.1448. ^{1}H NMR (270 MHz, $CDCl_3$, 21.4 °C) δ (parallel): 9.25 (dd, ^3J = 4.3 Hz, ^4J = 1.7 Hz, 2 H, $C(2,9)_{phen}$-*H*), 8.17 (dd, ^3J = 8.3 Hz, ^4J = 1.7 Hz, 2 H, $C(4,7)_{phen}$-*H*), 7.64 (dd, ^3J = 8.3 Hz, ^3J = 4.3 Hz, 2 H, $C(3,8)_{phen}$-*H*), 7.46−7.24 (m, C_{phenyl}-*H*, 10 H), 7.04 (s, 1 H, $C_{thiophene}$-*H*), 2.09 (s, 6 H, $C_{thiophene}-CH_3$) ppm; δ (antiparallel): 9.25 (dd, ^3J = 4.3 Hz, ^4J = 1.7 Hz, 2 H, $C(2,9)_{phen}$-*H*), 8.09 (dd, ^3J = 8.3 Hz, ^4J = 1.7 Hz, 2H, $C(4,7)_{phen}$-*H*), 7.62 (dd, ^3J = 8.3 Hz, ^3J = 4.3 Hz, 2 H, $C(3,8)_{phen}$-*H*), 7.46−7.24 (m, C_{phenyl}-*H*, 10 H), 7.02 (s, 1 H, $C_{thiophene}$-*H*), 2.16 (s, 6 H, $C_{thiophene}-CH_3$) ppm. ^{13}C NMR (100.6 MHz, $CDCl_3$, 21.4 °C) δ (parallel): 150.3, 145.9 (C_q), 140.6 (C_q), 136.8(C_q), 135.3 (C_q), 135.1, 134.3 (C_q), 133.2 (C_q), 129.0, 128.5 (C_q), 127.4, 126.6, 125.7, 125.3, 123.4, 14.4 (CH_3) ppm; δ (antiparallel): 150.3, 146.0 (C_q), 140.6 (C_q), 136.4(C_q), 135.2 (C_q), 135.0 (C_q), 134.2 (C_q), 133.1, 128,9, 128.7 (C_q), 127.4, 126.6, 125.7, 125.5, 123.4, 14.5 (CH_3) ppm.

*[Fe^{II}(H$_2$B(pz)$_2$)$_2$**L2**] (**2**).* A solution of potassium bis(1-pyrazolyl)-borohydride (0.34 g, 2.0 mmol) in dry MeOH (9 mL) was added dropwise to a stirred dry MeOH solution (5 mL) of $FeSO_4{\cdot}7H_2O$ (0.25 g, 1.0 mmol) at RT, whereupon a very fine white solid precipitated. The solid was removed by centrifugation followed by a decantation of the colorless solution of the in situ formed "$[Fe^{II}(H_2B(pz)_2)_2]$" (pz = 1-pyrazolyl). To this solution, **L2** (0.40 g, 1.0 mmol) dissolved in dry MeOH (30 mL) was added, and the resulting violet suspension was stirred for 2.5 h at RT. The suspension was concentrated to ∼1/3 volume and stored at −35 °C for 2 d. The violet precipitate was filtered off, washed with degassed water, and dried in vacuo to give **2** as a fine violet powder. Yield: 0.53 g, 76%. Anal. Calcd for $C_{38}H_{40}B_2FeN_{10}S_2$: C 58.64, H 5.18, N 17.99, S 8.24; found: C 58.57, H 5.19, N 17.97, S 8.23%. HRMS (ESI+): *m*/*z* calcd. for $[M-BH_2(pz)_2]^+$ 631.1573, found 631.1585; for $[M-BH_2(pz)_2$ + **L2**$]^+$ 1059.2959, found 1059.2982. Crystals suitable for X-ray structure determination were obtained upon slow diffusion of hexane into a toluene solution of **2** under inert atmosphere.

*[Fe^{II}(H$_2$B(pz)$_2$)$_2$**L3**] (**3**).* A solution of potassium bis(1-pyrazolyl)-borohydride (0.141 g, 0.76 mmol) in dry, degassed MeOH (5 mL) was added slowly to a solution of $FeSO_4{\cdot}7H_2O$ (0.106 g, 0.38 mmol) in dry, degassed MeOH (3 mL) at RT under inert gas atmosphere. After it was stirred for 10 min, the white precipitate was removed by centrifugation. The colorless solution of in situ formed "$[Fe^{II}(H_2B(pz)_2)_2]$" was decanted into a Schlenk tube, and a solution of **L3** (0.200 g, 0.38 mmol) in dry, degassed MeOH (16 mL) was added via cannula. The resulting violet suspension was stirred for 3 h at RT before it was stored at −35 °C for 3 d. The fine violet precipitate was filtered off, washed with degassed water, and dried in vacuo to yield **3** as a violet powder. Yield: 202 mg, 61%. Anal. Calcd for $C_{46}H_{40}B_2FeN_{10}S_2$: C 63.18, H 4.61, N 16.02, S 7.33; found: C, 62.64; H, 4.49; N, 15.80; S, 7,43%. HRMS (ESI+): *m*/*z* calcd. for $[M-BH_2(pz)_2]^+$ 727.1574, found 727.1557; for $[M-BH_2(pz)_2$ + **L3**$]^+$ 1251.2962, found 1251.2933. Crystals suitable for X-ray structure determination were obtained upon slow diffusion of hexane into a toluene solution of **3** under inert atmosphere.

X-ray Crystallographic Data Collection and Refinement of the Structures. Suitable crystals were embedded in protective perfluoropolyalkyl ether oil and transferred to the cold nitrogen gas stream of the diffractometer. Intensity data for **L2** were collected at 100 K, for **2** at 100 and 283 K, and for **3** at 100 and 273 K on a Bruker Kappa APEX2 *IμS* Duo diffractometer equipped with Quazar focusing Montel optics (Mo Kα radiation, λ = 0.710 73 Å). Data were corrected for Lorentzian and polarization effects; semi empirical absorption corrections were applied on the basis of multiple scans by using SADABS.[42] The structures were solved by direct methods and refined by full-matrix least-squares procedures on F^2 by using SHELXTL NT 6.12.[43] All non-hydrogen atoms were refined with anisotropic displacement parameters. Hydrogen atoms were placed in position of optimized geometry, and their isotropic displacement parameters were tied to those of their corresponding carrier atoms by a factor of 1.2 or 1.5. The crystallographic data, data collection, and structure refinement details are summarized in Table S1 (Supporting Information).

The diffraction data collected on the investigated crystal of **L2** rendered the molecule in the monoclinic space group $P2_1/n$ with two molecules of CH_3OH per formula unit. One of the CH_3OH solvent molecules was disordered. Two alternative orientations were refined resulting in site occupancies of 88.9(6) and 11.1(6)% for the atoms O1, C27 and O1A, C27A, respectively. SIMU and ISOR restraints were applied in the refinement of the disordered atoms.

The crystals of **2** contained four molecules per unit cell with two molecules of toluene per formula unit in the monoclinic space group $P2_1/n$. At 100 K one of the thiophene groups was disordered, and two alternative orientations were refined, resulting in site occupancies of 75(2) and 25(2)% for the atoms S2, C21−C26 and S2A, C21A−C26A, respectively. The disorder in one of the thiophene rings in **2** was also found at 283 K and refined for two different orientations with site occupancies of 61(2) and 39(2)% for the atoms S2, C21−C26 and S2A, C21A−C26A, respectively. At 283 K one of the toluene molecules also suffered from disorder. Two alternative orientations were refined and resulted in site occupancies of 62(2) and 38(2)% for the atoms C101−C107 and C111−C117, respectively. Similarity and pseudoisotropic restraints were applied to the anisotropic displacement ellipsoids of the disordered atoms.

DOI: 10.1021/acs.inorgchem.7b01952
Inorg. Chem. XXXX, XXX, XXX−XXX

The complex **3** crystallized with a total of 1.5 molecules of toluene per formula unit in the triclinic space group $P\bar{1}$. Half a toluene molecule was situated on crystallographic inversion center showing a disorder of the methyl group. The other toluene molecule was also disordered. Two alternative orientations were refined and resulted in site occupancies at 100 K of 62.1(4) and 37.9(4)% for the atoms C101−C107 and C111−C117, respectively. In the structure obtained at 273 K, those site occupancies were 37.9(6) and 62.1(6)%. Similarity and pseudoisotropic restraints were applied to the anisotropic displacement parameters of the disordered atoms.

RESULTS AND DISCUSSION

Synthesis and Crystal Structures. Novel photoactive diarylethene-based ligands **L2** and **L3** were obtained through multistep syntheses (Scheme 2). 3,8-Dimethyl-1,10-phenanthroline[34] was brominated in oleum to give a 5,6-dibromo derivative. The latter was C−C coupled with 2 equiv of (2,5-dimethylthiophen-3-yl)boronic acid, which was obtained from 2,5-dimethylthiophene in two steps,[35,36] to give **L2**. A similar route was used to synthesize **L3**. In the final step, 5,6-dibromo-1,10-phenanthroline[40] was reacted in a Suzuki cross-coupling reaction with 2 equiv of (2-methyl-5-phenylthiophen-3-yl)-boronic acid, which was obtained in two steps from 3,5-dibromo-2-methylthiophene,[38,39] to yield **L3**.

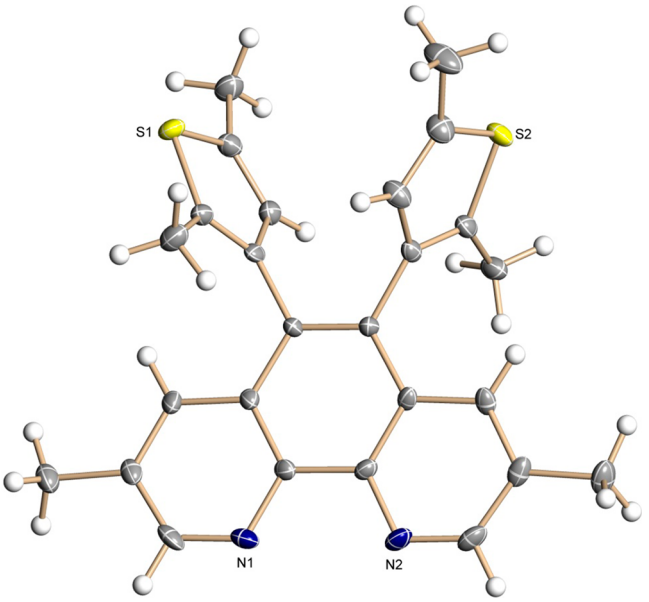

Figure 1. Molecular structure of open-ring **L2-o** in the antiparallel conformation at 100 K. Thermal ellipsoids are drawn at the 50% probability level.

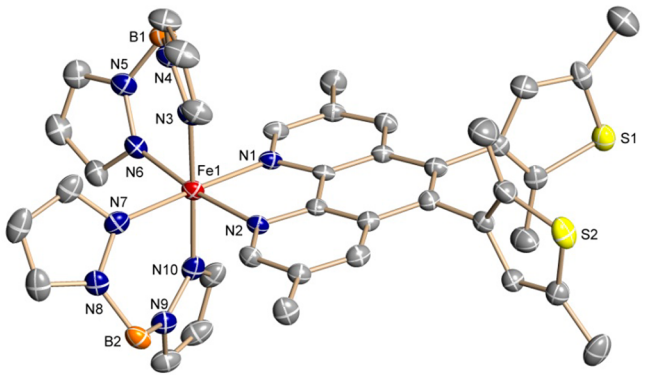

Figure 2. Molecular structure of open-ring **2-o** at 100 K showing an antiparallel conformation. The H atoms are omitted for clarity; the thermal ellipsoids are drawn at the 50% probability level.

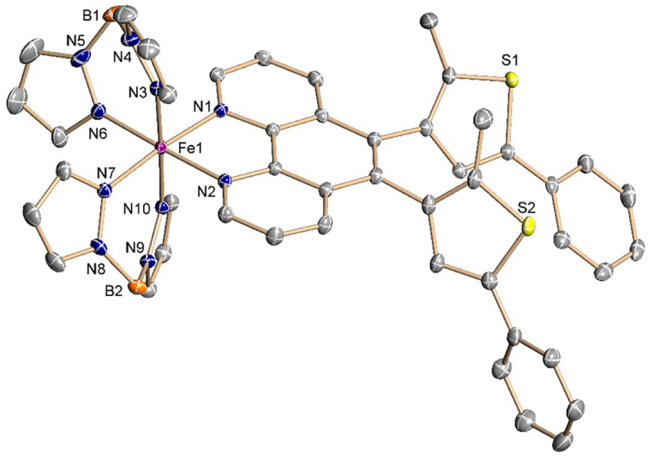

Figure 3. Molecular structure of open-ring **3-o** at 100 K showing a parallel conformation. The H atoms are omitted for clarity; the thermal ellipsoids are drawn at the 50% probability level.

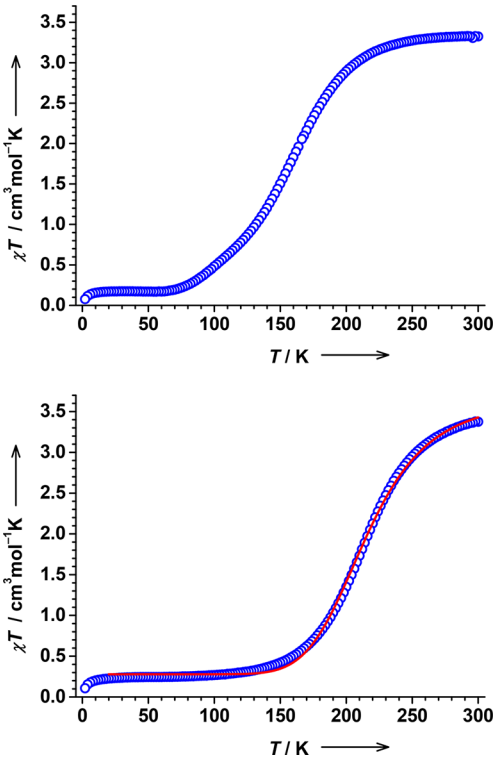

Figure 4. Variable-temperature χT products of **2** (top) and **3** (bottom) measured on powder samples at an external magnetic field of 1 T in the cooling mode (1 K min^{-1}, 2 K intervals). See the text for the fit parameters.

Generally, open-ring diarylethenes can adopt two conformations differing in mutual orientation of aryl (thiophene) fragments: a *photoactive antiparallel* conformer featuring a C_2 rotation axis and a *photoinactive parallel* conformer featuring a mirror plane.[44] Since the rotation along C(phenanthroline)−C(thiophene) bonds in **L1**−**L3** is sterically hindered and thus the interconversion between the conformers is slow, both conformers can be observed in solution at RT at the NMR time

DOI: 10.1021/acs.inorgchem.7b01952
Inorg. Chem. XXXX, XXX, XXX−XXX

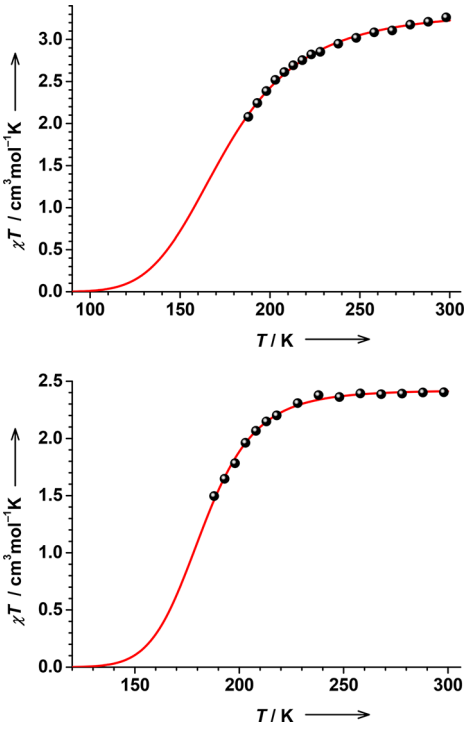

Figure 5. Variable-temperature χT products of **2** (top) and **3** (bottom) measured in toluene solutions with the Evans NMR method (toluene/toluene-d_8/TMS = 10:2:1). van't Hoff fit parameters for **2**: ΔH = 11.2(7) kJ mol^{-1}, ΔS = 64(4) J K^{-1}; for **3**: ΔH = 22(1) kJ mol^{-1}, ΔS = 119(7) J K^{-1}.

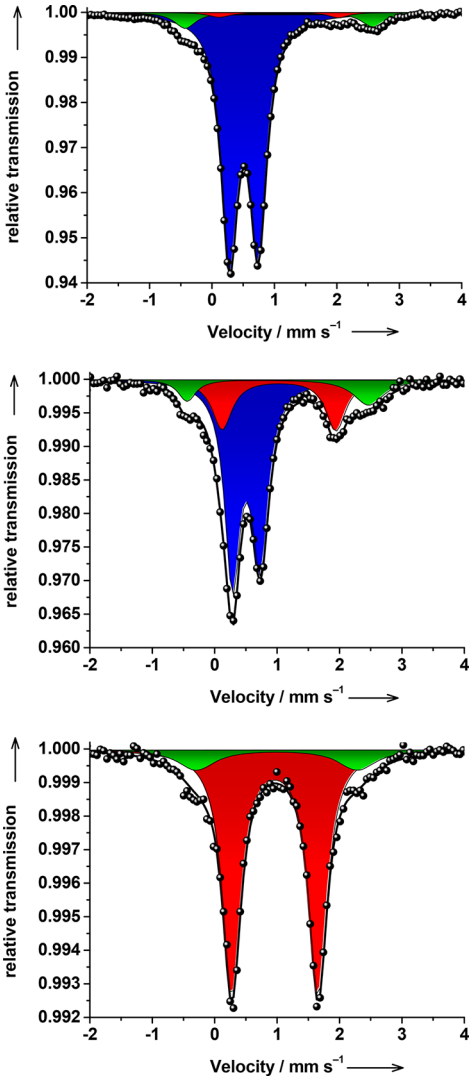

Figure 6. Zero-field ^{57}Fe Mössbauer spectra measured on **2** at 78 (top), 150 (middle), and 297 K (bottom). Relative intensities: (top) 90% LS-Fe(II) in blue, 2% HS-Fe(II) in red, 8% minor HS-Fe(II) in green; (middle) 65% LS-Fe(II) in blue, 22% HS-Fe(II) in red, 13% minor HS-Fe(II) in green; (bottom) 85% HS-Fe(II) in red, 15% minor HS-Fe(II), in green. See the text and Supporting Information for the fit parameters.

scale. Thus, similarly to the parent **L1** ligand,[23,45] two sets of signals are observed in ^{1}H NMR spectra of **L2** and **L3**. Importantly, a mixture containing both conformers at ∼1:1 ratio is usually obtained in the Suzuki reaction (vide supra). However, because of slightly differing solubility and retention factors, after workup, we often obtain a mixture enriched for one or another conformer. This allows the assignment of signals in ^{1}H NMR spectra to different conformers (see Experimental Section and Supporting Information). For example, the CH_3 protons of **L3** resonating at 2.09 (parallel) and 2.16 (antiparallel) ppm are clearly distinguishable.

In the context of photoswitching, samples that are enriched for or contain exclusively a photoactive antiparallel conformer are preferred.[46,47] However, we noticed that the samples of **L1**−**L3** enriched significantly for one or another conformer convert slowly and spontaneously to an ∼1:1 mixture in solution at RT. The interconversion between the conformers can be further accelerated by heating or ultrasonic waves. We assume that similar effects are operative for the ligands within the complexes **1**−**3**. As an important consequence, the exact ratio between the conformers in photoexperiments in solutions (vide infra) is not known.

The crystallization from a methanolic solution rendered colorless crystals of **L2** suitable for X-ray structure determination (Figure 1). The open-ring isomer (**L2-o**) crystallized in the monoclinic $P2_1/n$ space group with four molecules of the ligand molecules together with eight MeOH solvates per unit cell. The picked crystal contained exclusively an antiparallel conformer[44] with α-methyl groups (relative to C−C thiophene-phenanthroline bond) pointing to opposite directions. At 100 K, the thiophene rings form dihedral angles of 74.2 and 75.1° with a nearly planar phenanthroline unit. Hence, the π-systems of the two thiophene moieties and the phenanthroline backbone in **L2-o** are essentially electronically uncoupled. A similar orthogonality of those units was observed for a parent **L1-o** ligand.[45]

Colorless methanolic solutions of **L2** and **L3** reacted immediately with a colorless methanolic solution of "[Fe^{II}(H$_2$B(pz)$_2$)$_2$]", which was generated in situ from K(H$_2$B(pz)$_2$),[37] forming deep purple precipitates of the target paramagnetic complexes **2** and **3**, respectively. While the dried powders of **2** and **3** were used for all subsequent physical and photophysical studies, small amounts of crystalline materials were obtained upon slow diffusion of *n*-hexane into toluene solutions of the complexes. The crystals were suitable for X-ray structure determination, which was accomplished at 100 and 283 K for **2**, and at 100 and 273 K for **3**.

The complex **2** crystallized in the monoclinic $P2_1/n$ space group with four molecules of open-ring **2-o** and eight molecules of toluene per unit cell. Two $(H_2B(pz)_2)^{-1}$ and one **L2-o**

DOI: 10.1021/acs.inorgchem.7b01952
Inorg. Chem. XXXX, XXX, XXX−XXX

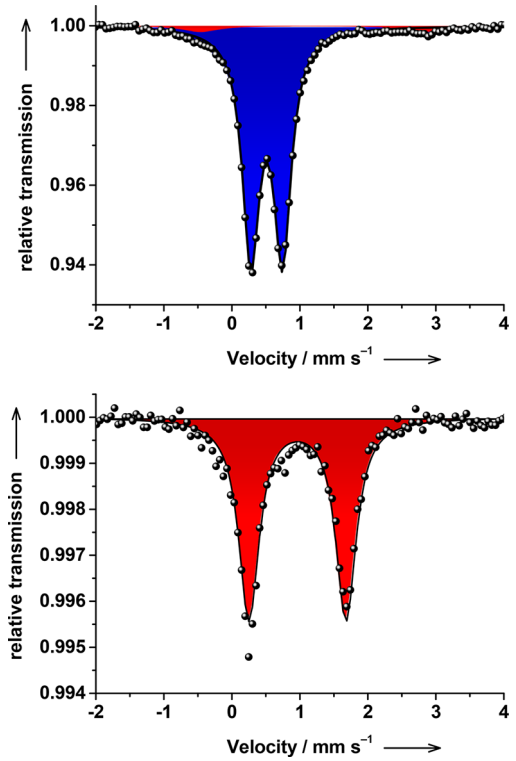

Figure 7. Zero-field ^{57}Fe Mössbauer spectra measured on **3** at 77 (top) and 298 K (bottom). Relative intensities: (top) 95% LS-Fe(II) in blue, 5% HS-Fe(II) in red; (bottom) 100% HS-Fe(II) in red. See the text and Supporting Information for the fit parameters.

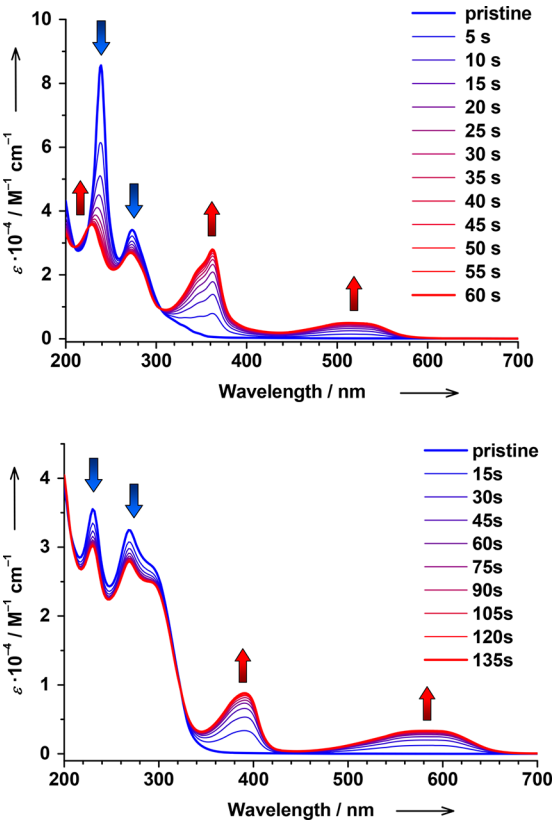

Figure 8. Photocyclization of **L2-o** (top) and **L3-o** (bottom) with UV light at RT (λ = 282 nm, MeCN solutions, c = 6.0 × 10^{-5} M).

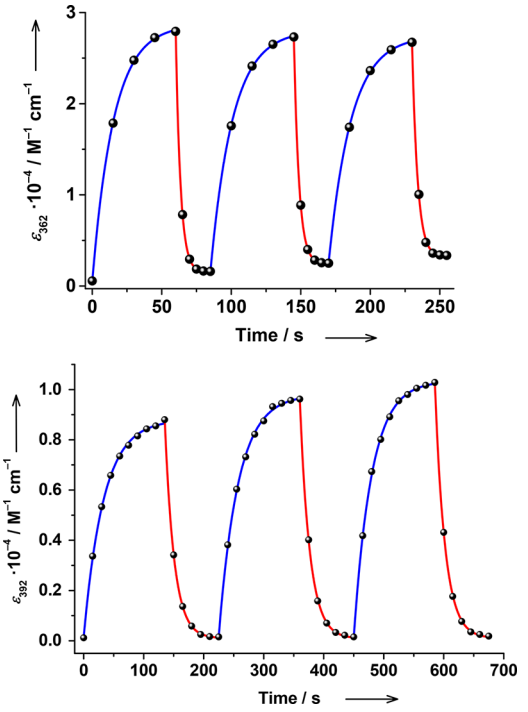

Figure 9. Multiple photoswitching of **L2** (top) and **L3** (bottom) in MeCN solutions at RT (c = 6.0 × 10^{-5} M). The evolution of the 362 and 392 nm absorption, respectively, upon alternating photocyclization with λ = 282 nm (blue) and photocycloreversion with visible ($\lambda \geq$ 400 nm, red). The data were fitted according to the first-order kinetics.

ligands form a distorted N_6 coordination environment around the iron(II) central ion (Figure 2). At 100 K, **2-o** shows relatively short Fe−N bond distances in the range of 2.030(2)−2.058(2) Å indicative of an LS-Fe(II) ion.[48,49] One of the thiophene rings is disordered showing two alternative orientations with site occupancies of 75(2) and 25(2)%. Interestingly, both orientations represent photoactive antiparallel conformers. The major orientation (75%) reveals dihedral angles between the thiophene rings and phenanthroline backbone of 88.1 and 89.3°, while the corresponding angles in the alternative orientation (25%) are 88.1 and 84.9°. Consequently, the electronic conjugation between the π-systems of the phenanthroline and two thiophenes is negligible. Interestingly, in the previously reported crystal structures of **1-o**,[23,50] the thiophenes and phenanthroline backbone are slightly less orthogonal showing dihedral angles in the range of 61.8−84.0°.

At 283 K the space group is preserved. However, all Fe−N bond distances increased significantly to 2.147(4)−2.221(4) Å, which is typical for HS-Fe(II) complexes.[13,48,49,51] Thus, similar to a powder sample (vide infra), the crystals of **2-o** show thermally induced SCO. Similar to the low-temperature structure, one thiophene is disordered resulting in two alternative orientations with site occupancies of 61(2) and 39(2)% at 283 K. Both orientations are antiparallel conformers. The thiophenes are nearly orthogonal to the phenanthroline plane confirmed by the corresponding dihedral angles of 84.8−89.5°.

The complex **3** crystallized in the triclinic $P\bar{1}$ space group with two molecules of open-ring **3-o** and three molecules of toluene per unit cell. The coordination environment of **3-o** (Figure 3) is very similar to **2-o**. At 100 K, **3-o** is in an LS-

DOI: 10.1021/acs.inorgchem.7b01952
Inorg. Chem. XXXX, XXX, XXX−XXX

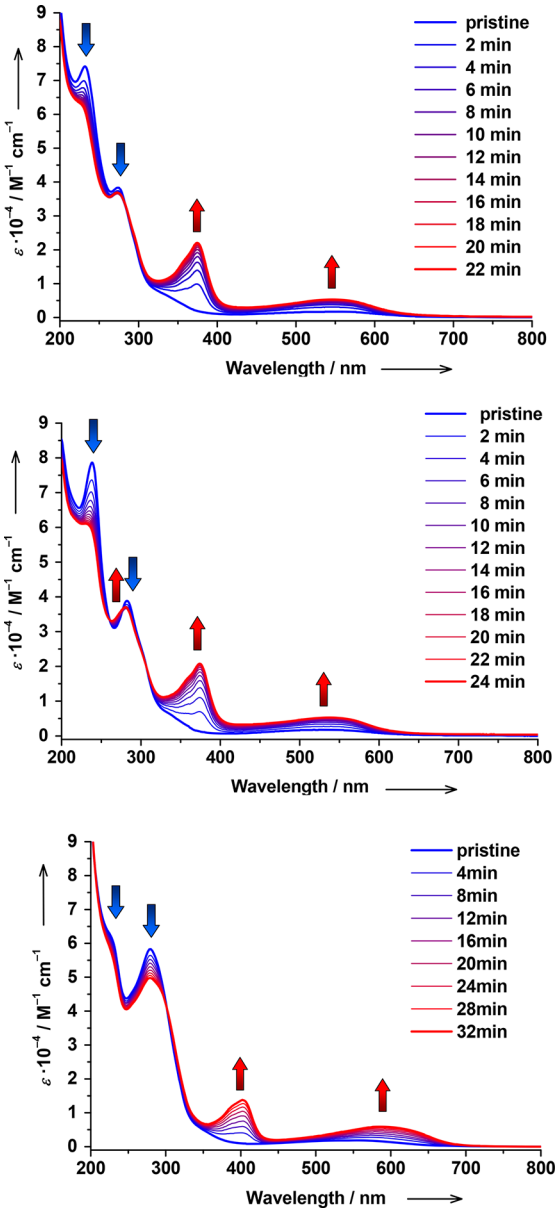

Figure 10. Photocyclization of **1-o** (top), **2-o** (middle), and **3-o** (bottom) with UV light at RT (λ = 282 nm, MeCN solutions, c = 1.3 × 10^{-5} M).

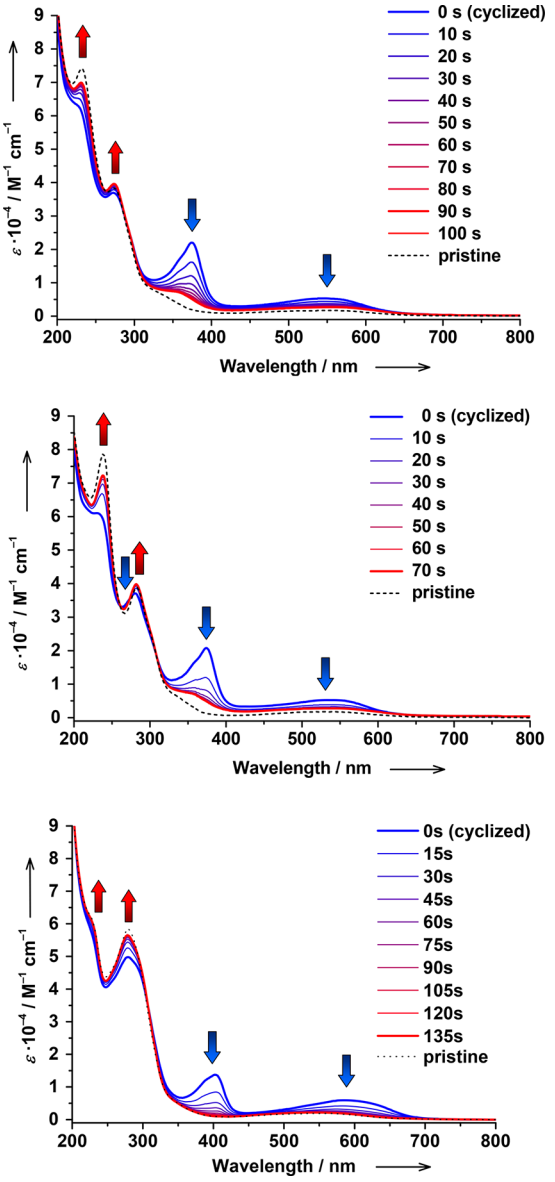

Figure 11. Photocycloreversion of **1** (top), **2** (middle), and **3** (bottom) with visible light at RT ($\lambda \geq 400$ nm, MeCN solutions, c = 1.3 × 10^{-5} M) starting from photocyclized solutions (λ = 282 nm).

Fe(II) state confirmed by short Fe−N distances in the range of 1.9715(14)−2.0237(15) Å. Interestingly, the picked crystal contained exclusively parallel conformer this time. Note that, which conformer crystallizes out of solution usually containing both conformers, depends on crystallization conditions. Thus, different conformers can be crystallized from the same starting mixed material as was demonstrated for **1-o**.[23,50] The dihedral angles between the thiophene rings and phenanthroline backbone of 57.9 and 67.7° in **3-o** are smaller compared with **1-o** and **2-o**. The phenyl substituents are not coplanar with the corresponding thiophene fragments but moderately turned by 29.0 and 38.6° in the crystal.

At 273 K the space group is preserved, but all Fe−N bond distances increased significantly to 2.151(2)−2.229(2) Å confirming a thermally induced transition to an HS-Fe(II) state. The dihedral angles between the thiophene units and phenanthroline backbone at 59.2 and 70.4° are slightly increased compared to the low-temperature structure. The phenyl substituents are twisted relative to the corresponding thiophene units by 30.0 and 37.1° in the HS structure.

Magnetic Properties. Variable-temperature magnetic susceptibility measurements were performed on as-synthesized powder samples of **1**−**3** in the temperature range of 2−300 K. A nearly constant χT product of 3.33 cm^3 mol^{-1} K (χ is molar magnetic susceptibility; see Supporting Information for effective magnetic moment) at 280−300 K measured for **2** confirms an HS-Fe(II) state (Figure 4). When slowly cooled (1 K min^{-1}, 2 K intervals), the χT product decreases gradually to 0.17 cm^3 mol^{-1} K at 64 K, which reflects a thermally induced HS→LS transition. A low-temperature plateau (16−64 K) is indicative of a nearly complete SCO with a residual HS fraction of 5%. At temperatures below 16 K, the χT product decreases further reaching 0.08 cm^3 mol^{-1} K at 2 K, which is likely due to the zero-field splitting of the residual HS fraction. When slowly heated from 2 to 300 K, the data coincide with those obtained

DOI: 10.1021/acs.inorgchem.7b01952
Inorg. Chem. XXXX, XXX, XXX−XXX

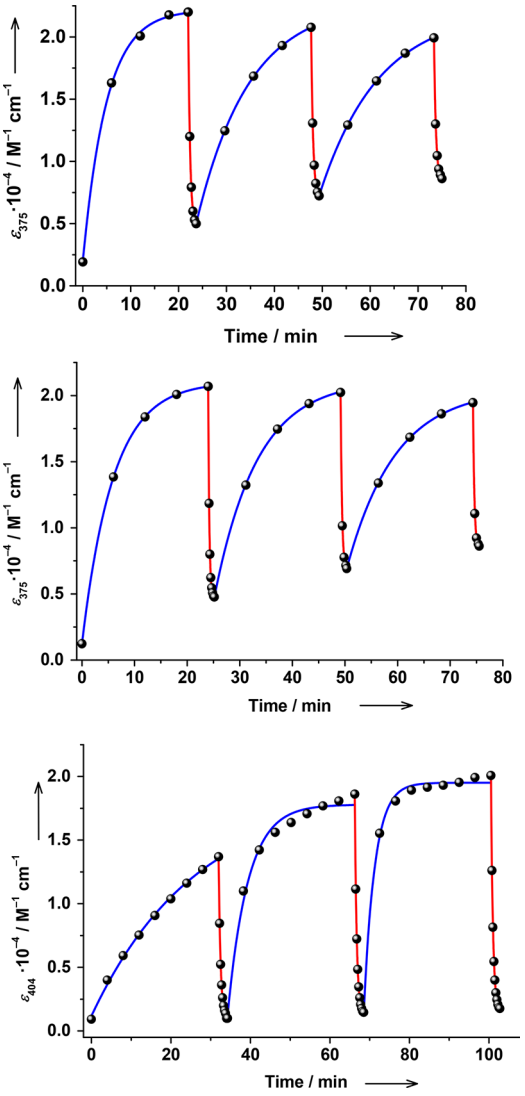

Figure 12. Multiple photoswitching of **1** (top), **2** (middle), and **3** (bottom) in MeCN solutions ($c = 1.3 \times 10^{-5}$ M) at RT. The evolution of the absorption at 375 (**1**, **2**) and 404 (**3**) nm upon alternating photocyclization with λ = 282 nm (blue) and photocycloreversion with visible ($\lambda \geq 400$ nm, red). The data were fitted according to the first-order kinetics.

in the cooling mode, and thus no thermal hysteresis could be detected.

Interestingly, **2** shows a two-step SCO transition with transition temperatures $T_{1/2}$ of ~102 and 160 K as estimated from the first derivative d(χT)/dT (Supporting Information). Generally, a two-step SCO might be due to the presence of two nonequivalent complex molecules in the crystal cell or the formation of HS/LS pairs upon transition due to short-range interactions.[52] A possible disorder or the simultaneous presence of antiparallel and parallel conformers could be responsible for the two-step transition as well. Note that the magnetic measurements made on the powder sample obtained from a MeOH solution are not directly comparable with the X-ray structural data from few crystals obtained from a toluene/*n*-hexane solution (see Supporting Information for powder XRD data). Our attempts to crystallize **2** from MeOH were unfortunately unsuccessful.

Complex **3** reveals a χT product of 3.38 cm^3 mol^{-1} K at 300 K. When slowly cooled, the χT product decreases gradually to

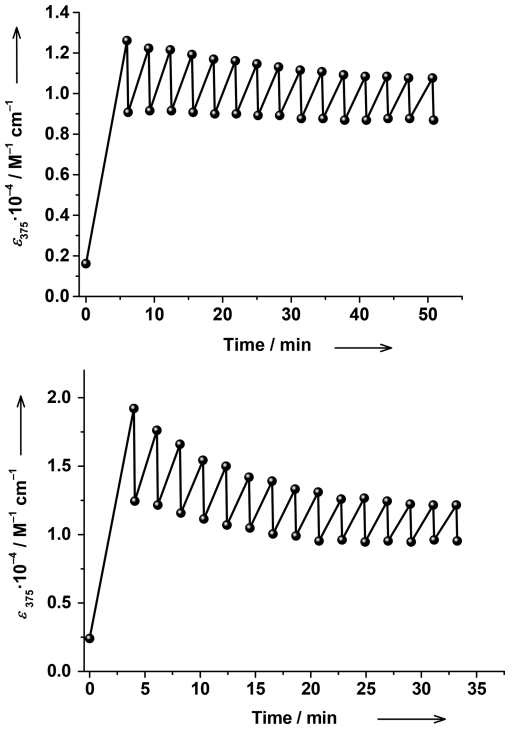

Figure 13. Multiple photoswitching of **1** (top) and **2** (bottom) in MeCN solutions ($c = 1.3 \times 10^{-5}$ M) at RT. The evolution of the absorption at 375 nm upon alternating photocyclization with λ = 282 nm (increasing absorption) and photocycloreversion with visible ($\lambda \geq$ 400 nm, decreasing absorption).

0.25 cm^3 mol^{-1} K measured at 70 K disclosing a thermally driven SCO (Figure 4). When further cooled, the χT product remains nearly constant followed by a drop at very low temperatures due to the zero-field splitting of the residual HS fraction (7%). No hysteresis was observed upon subsequent heating. In contrast to **2**, complex **3** reveals a clear one-step SCO transition. This was readily fitted using the van't Hoff eq 1 to give the enthalpy change ΔH = 15.9(3) kJ mol^{-1} and entropy change ΔS = 74(2) J K^{-1} mol^{-1} for the LS→HS conversion (χ_{LT} and χ_{HT} are low- and high-temperature limits for molar magnetic susceptibility, respectively).

$$\chi T = \frac{\chi_{LT} T + \chi_{HT} T \exp(-\Delta H + T\Delta S/RT)}{1 + \exp(-\Delta H + T\Delta S/RT)} \quad (1)$$

Similar thermodynamic parameters were previously determined for **1** (10.2(4) kJ mol^{-1} and 76(3) J K^{-1} mol^{-1}).[23] The transition temperature $T_{1/2}$ for **3** was calculated at 215.7(5) K. This is the highest temperature in the series of **1**–**3**. Note that the influence of electronic factors on $T_{1/2}$ values is best examined in solutions, where intermolecular interactions are negligible (vide infra).

For consistency, we reinvestigated[23,24,53] the magnetic properties of **1** under similar experimental conditions (1 K min^{-1}, 2 K intervals, Supporting Information). The inspection of the d(χT)/dT derivative confirms a simple one-step SCO transition in **1**. The obtained thermodynamic parameters: ΔH = 11.8(3) kJ mol^{-1}, ΔS = 86(2) J K^{-1}, and the corresponding transition temperature $T_{1/2}$ = 136.9(3) K, resemble closely the values obtained previously from the lower-quality data.[23]

Magnetic properties of newly synthesized complexes **2** and **3** were investigated in solution using the Evans NMR method

DOI: 10.1021/acs.inorgchem.7b01952
Inorg. Chem. XXXX, XXX, XXX−XXX

(Figure 5) and compared with the previously reported data on **1**. The χT product of 3.26 cm^3 mol^{-1} K measured for **2** at RT in toluene solution is very close to the value observed in the solid state (3.33 cm^3 mol^{-1} K). For **3**, the χT product at RT in toluene is smaller than in the solid sample. Importantly, both **2** and **3** reveal a gradual HS→LS transition upon cooling from RT to 188 K. The temperature-dependent data were readily fitted with the van't Hoff equation, and the thermodynamic parameters for SCO were obtained (Figure 5). Note that the calculated transition temperatures of 175.2(6) and 182.5(4) K for solutions of **2** and **3**, respectively, are higher than $T_{1/2}$ of **1** determined at 164(1) K.[23] Thus, the LS state is stabilized in the series: **3** > **2** > **1**.

Mössbauer Spectroscopy. Zero-field ^{57}Fe Mössbauer spectra obtained on a powder sample of **2** at different temperatures confirm a thermally driven SCO (Figure 6). The RT spectrum reveals a major doublet (85%) with an isomer shift (δ) of 0.97 mm s^{-1} and a quadrupole splitting ($|\Delta E_Q|$) of 1.38 mm s^{-1}, which is assigned to a HS-Fe(II) state. A minor doublet (15%) shows a very similar isomer shift but much larger quadrupole splitting of 2.58 mm s^{-1}, which is due to a HS-Fe(II) species. When cooled to T = 105 K, the relative intensity of the major doublet decreases to 22% with concomitant appearance of an LS-Fe(II) species (65%) featuring δ = 0.51 mm s^{-1} and $|\Delta E_Q|$ = 0.44 mm s^{-1}. Thus, the major component in the powder sample of **2** is SCO active. Interestingly, the relative intensity of the minor HS-Fe(II) doublet remains nearly constant (13% at 105 K), which confirms that the minor species is trapped in an HS state at these temperatures. Finally, at T = 78 K, the thermally induced SCO is nearly completed, which is confirmed by the presence of 90% of LS-Fe(II) species, 2% of SCO HS-Fe(II) species, and 8% of a minor HS-Fe(II) species. The minor HS-Fe(II) species showing a very similar to the major species isomer shift but differing quadrupole splitting is likely due to slightly differing environment of **2** in two different lattices, rather than due to impurities.

Complex **3** shows a single quadrupole doublet with δ = 0.96 mm s^{-1} and $|\Delta E_Q|$ = 1.43 mm s^{-1} at RT (Figure 7). These parameters resemble closely those of the HS-Fe(II) state of **2** (vide supra). When cooled to 77 K, the HS doublet nearly disappears, and a new doublet with δ = 0.51 mm s^{-1} and $|\Delta E_Q|$ = 0.46 mm s^{-1} appears (95%), which is due to the thermal switching to the LS-Fe(II) state. Interestingly, a small amount of an HS species (5%) present at 77 K shows distinctly different Mössbauer parameters (δ = 1.19 mm s^{-1} and $|\Delta E_Q|$ = 3.30 mm s^{-1}) compared to the HS species at RT. Although the fit parameters of the HS species at 77 K should be considered with care due to its very weak signal (Figure 7), we suggest that this species is a minor impurity rather than a residual HS fraction of the SCO complex **3**. Overall, the variable-temperature Mössbauer data obtained on **2** and **3** are in very good agreement with the magnetic measurements on the corresponding solids (vide supra).

Electronic Absorption Spectroscopy. Both novel ligands **L2-o** and **L3-o** form colorless solutions in MeCN, and their electronic absorption spectra have no features in the visible. The spectrum of **L2-o** shows two strong bands in the UV at 238 ($\varepsilon = 8.7 \times 10^4$ M^{-1} cm^{-1}) and 274 nm ($\varepsilon = 3.4 \times 10^4$ M^{-1} cm^{-1}) with a shoulder at 330 nm (Supporting Information). These bands are bathochromically shifted relative to very similar bands of **L1-o** (232 and 267 nm, respectively),[23] which were assigned to intraligand $\pi \rightarrow \pi^*$ and $n \rightarrow \pi^*$ transitions of the phenanthroline framework and the thiophene moieties.[45] The spectrum of **L3-o** is clearly different. The spectrum features two strong bands at 230 and 269 nm of nearly equal intensity (ε = 3.6 and 3.3 × 10^4 M^{-1} cm^{-1}, respectively), with a shoulder at ∼300 nm becoming more pronounced.

In the UV region, the complexes **2-o** and **3-o** show the absorption bands similar to the corresponding ligands (Supporting Information). The spectrum of **2-o** reveals two strong bands at 237 ($\varepsilon = 7.4 \times 10^4$ M^{-1} cm^{-1}) and 281 nm ($\varepsilon = 3.8 \times 10^4$ M^{-1} cm^{-1}) with a shoulder, whereas **3-o** features an unresolved structure at wavelengths less than 230 nm and a strong band at 280 nm ($\varepsilon = 5.8 \times 10^4$ M^{-1} cm^{-1}) with a shoulder. Note that the low-energy UV bands of the complexes are bathochromically shifted compared with those of the corresponding metal-free ligands due to coordination. The visible region is dominated by a broad relatively low-intense metal-to-ligand charge transfer (MLCT) band at ∼550 nm ($\varepsilon \approx 0.2 \times 10^4$ M^{-1} cm^{-1}) for both complexes.

Photophysical Properties of Ligands. Upon UV irradiation at λ = 282 nm, a colorless solution of **L2-o** became rapidly red. Thereby the prominent absorption bands in UV region decreased in intensity, and the new bands at 362 (with a shoulder) and 512 nm appeared (Figure 8). These changes are characteristic for the photocyclization of diarylethenes,[44] and very similar spectral changes were reported for the photocyclization of **L1-o**.[23] As expected, the photoreaction follows a simple first-order kinetics (Supporting Information). The photocyclization of **L2-o** was accomplished within 60 s. The photostationary state (PSS) is characterized by the presence of 63% of open-ring and 37% of closed-ring isomers, as determined by NMR spectroscopy (Supporting Information). Irradiation of **L2-o** at λ = 254 nm yielded a very similar PSS (Supporting Information).

The photocyclization of the colorless solution of **L3-o** with λ = 282 nm gave a blue solution. Upon UV irradiation, the parent absorption bands in UV decreased in intensity, whereas the new bands at 392 and 584 nm emerged (Figure 8). The new bands are bathochromically shifted compared to **L2**. The degree of open-ring→closed-ring photoconversion was difficult to determine here, because of a limited thermal stability of the closed-ring isomer at RT (vide infra). Interestingly, the photocyclization of **L3-o** with λ = 254 nm resulted in a slightly high degree of photoconversion compared to the excitation at λ = 282 nm, as confirmed by the electronic absorption spectroscopy (Supporting Information).

For consistency, we reinvestigated the photocyclization of **L1-o** under similar conditions. The photoresponse of **L1-o** to λ = 282 nm (Supporting Information) is very similar to that of **L2-o** and to the previously reported photocyclization with λ = 254 nm UV source.[23]

The photocyclization of **L1**−**L3** was reversible. Upon irradiation with visible light at RT, the red (**L1**, **L2**) or blue (**L3**) solutions containing closed-ring ligands became colorless, and the parent electronic absorption spectra of the open-ring ligands were fully restored (Supporting Information). The photocycloreversion reactions proceed very fast under our experimental conditions: the reactions were completed within 25 and 90 s for **L1**/**L2** and **L3**, respectively.

An open-ring isomer is usually the ground state of a diarylethene and thus thermodynamically stable, whereas a higher-energy closed-ring isomer could be thermally stable for 1 × 10^5 years or for only several seconds at RT, depending on the particular type of a diarylethene and its substituents.[44] The half-

DOI: 10.1021/acs.inorgchem.7b01952
Inorg. Chem. XXXX, XXX, XXX−XXX

life of the parent ligand **L1-c** was estimated at 137 h in MeCN solution at RT.[23] Here we found that the introduction of methyl substituents into the phenanthroline backbone (**L2**) and phenyl substituents into thiophene moieties (**L3**) both decreased the thermal stability of the closed-ring isomers. Whereas the half-life of **L2-c** decreased only moderately to 42(1) h, **L3-c** became much less stable showing the half-life of only 11.99(3) min in MeCN solution at RT (Supporting Information).

We examined the unexpected decrease of the thermal stability of the substituted ligands by density functional theory (DFT) calculations. The activation barrier for a thermal cycloreversion reaction and thus the stability of a closed-ring isomer is expected to be reversely proportional to the energy difference between open- and closed-ring isomers.[54] Thus, we calculated open-ring/closed-ring energy differences for ligands **L1**−**L3** (Supporting Information). However, the energy differences were nearly the same (25.1−26.6 kcal mol^{-1}) for all ligands. Moreover, **L3** showed the smallest energy difference, and thus **L3-c** would be expected to be the most stable in the series, which is not confirmed experimentally.

Lehn et al. suggested that the strength of the photogenerated C−C bond in a closed-ring isomer could be an alternative indicator for its thermal stability.[55] Indeed, the calculated C−C bond in **L3-c** is slightly longer (1.537 Å) than in **L1-c** and **L2-c** (both 1.534 Å), confirming the lower stability of **L3-c**. However, this argument should be taken with care, since the π-systems of the two thiophenes and phenanthroline are all involved into the cyclization/reversion process. More insight regarding the influence of substituents on thermal stability might be obtained from transition states calculations,[56] which is beyond the scope of this work.

Further, we examined multiple photoswitching of **L1**−**L3** ligands. The ligands were photocyclized with UV light until the PSS was nearly reached, followed by the photocycloreversion with visible light until another PSS was attained. Afterward the cycle was repeated two more times, while the irradiation times were *kept constant*. All three ligands could be reversibly switched in MeCN solution at RT (Figure 9 and Supporting Information). Interestingly, whereas **L1** and **L2** showed a small degree of photodegradation, the photoswitchability of **L3** improved with every cycle. Thus, the photoconversion increased in every subsequent photocyclization step for **L3**. We ascribe this effect to the conversion of the photoinactive parallel conformer to the photoactive antiparallel conformer under UV irradiation. This is supported by the observation that, upon prolonged UV excitation, the rate of photocyclization becomes nearly constant (Supporting Information). As a consequence, the PSS for the photocyclization of **L3** is difficult to reach. Notably, the interconversion between the two conformers in solution is very slow without UV irradiation, as was determined by NMR spectroscopy. Therefore, we suggest that the irradiation at λ = 282 nm could induce $\pi \rightarrow \pi^*$ electronic transitions within phenyl substituents of **L3-o**, thus providing additional energy or new pathways that ultimately facilitate the interconversion between the conformers. Usually the conformers are tending to ∼1:1 ratio in solution, while only the antiparallel conformer is photoactive. The disturbed equilibrium between the conformers in the irradiated solution and the suggested UV-enhanced interconversion between the conformers should lead to the gradual conversion of parallel into antiparallel conformers.

Photophysical Properties of Complexes. After the reversible and multiple photoswitching of the metal-free ligands **L1**−**L3** at RT was confirmed (vide supra), we investigated the photoresponse of the corresponding iron(II) complexes **1**−**3**. Besides reporting the photophysical properties of the newly synthesized molecular switches **2** and **3**, here we reexamined[23] some properties of the parent switch **1** using a new photosetup employed for **2** and **3**.

Generally, the photoresponse of **1**−**3** is very similar to the corresponding free ligands. However, the photoreactions with the complexes proceed significantly slower, which points to decreased quantum yields for the coordinated diarylethenes. This is likely due to partial deactivation of diarylethene-based electronic excited states by charge transfer and metal-based ligand-field states. The UV-induced photocyclization in **1**−**3** is accompanied by the decrease of the prominent absorption bands in UV, and the appearance of the characteristic bands due to the closed-ring isomers (Figure 10). The new bands of the closed-ring **2-c** (**3-c**) are centered at 374 and 537 nm (402 and 586 nm). These are bathochromically shifted relative to those of the closed-ring ligands, which indicates that the diarylethene-based ligands remain coordinated to the metal ions.

The photocyclization of **2-o** proceeds very similar to that of **1-o** and follows the first-order kinetics (Supporting Information). Although the photocyclization of **3-o** could also be fitted to the first-order kinetics, upon prolonged UV irradiation the photocyclization rate becomes virtually constant (Supporting Information). A similar effect was observed for the photocyclization of the metal-free **L3-o** (vide supra). We ascribe this to the UV-enhanced interconversion between the parallel and antiparallel conformers of **3-o** in solution.

In our previous works, we showed that the reversible photocyclization of **1** triggers the reversible HS-to-LS transition at the iron(II) center. This unique SCO was accomplished in solution and in the solids state at RT, and the switching proceeds at the molecular level.[23,24] Note that the π-systems of the phenanthroline and the two twisted thiophenes are essentially electronically uncoupled in the open-ring **L1-o**. In contrast, the closed-ring **L1-c** becomes nearly planar that leads to the formation of a common π-system. Thus, we suggested that **L1-o** is a weaker π-acceptor, which produces a weaker ligand field thus stabilizing an HS state in **1-o**, whereas **L2-c** is a stronger π-acceptor, which produces a stronger ligand field thus stabilizing an LS state in **1-c**.[23]

Since the magnetic and photophysical properties of **2** are very similar to those of **1**, we expected that the photocyclization of **2** triggers an HS-to-LS transition as well. Indeed upon bulk photolysis of a concentrated solution of **2** in a MeCN/MeCN-d_3 mixture with UV light, the χT product decreased gradually from 2.86 to 2.33 cm^3 mol^{-1} K, as determined by the Evans NMR method. Thus, ∼19% of HS species were converted into LS species upon UV irradiation at RT. Prolonged irradiation with UV resulted in the photodegradation of the sample, as confirmed by electronic absorption spectroscopy. Similar photodegradation issues in longtime bulk photolysis experiments were noticed for **1**, for which the photoconversion of 40% was reported.[23]

The photocyclization of **1**−**3** is reversible. The photocycloreversion can be induced by selective irradiation into the emerging bands of the closed-ring isomers, or by unselective irradiation with visible light ($\lambda \geq$ 400 nm) at RT. Thus, upon irradiation, the bands of the closed-ring complexes decrease,

DOI: 10.1021/acs.inorgchem.7b01952
Inorg. Chem. XXXX, XXX, XXX−XXX

and the bands of the open-ring complexes increase in intensity (Figure 11). Note that the spectra of the pristine open-ring **1-o** and **2-o** are not fully restored, and thus the reverse reactions are not fully complete, which is due to nonzero absorption of the open-ring complexes in the visible.[23] In contrast, the photocycloreversion of **3** seems to be fully completed within 135 s, which is very likely due to very short lifetime of **3-c** (vide infra).

The thermal stability of SCO photoswitches **1**−**3** at RT, which is important for potential applications, was investigated in solutions. Similar to the free ligands, the open-ring complexes are thermodynamically stable, whereas the UV-generated closed-ring complexes show considerably different stability. The half-life of **1-c** was previously determined at 421 h (17.5 d) in solution at RT.[23] The thermal stability of **2-c** is only moderately lower; the respective half-life is 199(12) h (8.3(5) d, Supporting Information). However, **3-c** seems to be considerably less stable showing the half-life of only 3.3(2) min at RT. Thus, the stability of the closed-ring complexes, **1-c** > **2-c** ≫ **3-c**, follows the trend observed for the ligands: **L1-c** > **L2-c** ≫ **L3-c**. Consequently, the thermal stability of closed-ring ligands can be used as an indicator for the stability of prospective SCO complexes.

To test the resistance of SCO photoswitches **1**−**3** to fatigue, we performed three consecutive photocycles by irradiating the complexes with alternating UV and visible light in solution at RT. Importantly, the complexes were irradiated until the PSSs are reached during the first photocycle. Afterward, the times for UV and visible light irradiations were *kept constant*. Since the PSS at λ = 282 nm for **3** is difficult to reach (vide supra), this complex was photocyclized for 32 min in the first cycle, and this time was kept constant.

The photoswitches **1** and **2** show very similar properties. Upon every cycle, the photoresponse of these species diminishes pointing to slow photodegradation. This can be best followed by monitoring the prominent absorptions at 375 nm (Figure 12). For instance, the maximum of the extinction coefficient at 375 nm, ε_{375}, drops slightly from 2.07×10^4 M^{-1} cm^{-1} in the first cycle to 1.95×10^4 M^{-1} cm^{-1} in the third cycle for the photocyclized solution of **2**. Concomitantly, the minimum of ε_{375} achieved upon photocycloreversion increases significantly from 0.48×10^4 M^{-1} cm^{-1} after the first cycle to 0.86×10^4 M^{-1} cm^{-1} after the third cycle.

Complex **3** behaves differently. Similarly to the metal-free **L3**, the photoresponse of **3** seems to increase with every cycle (Figure 12). Although the origin of this enhancement is not fully understood, it is likely similar to the free ligand (vide supra). Thus, we assume that the relatively fast generation of additional amount of antiparallel conformers in UV-irradiated solution improves the response to UV, while the fast **L3-c**→**L3-o** thermal relaxation produces an apparent effect that the complex converts fully to the initial state upon irradiation with visible. Because of these effects, the data for **3** could only be roughly fitted according to the first-order kinetics.

During our studies, we noticed that the photodegradation of **1** and **2** increases in longtime photoexperiments and when the solutions are irradiated longer than required to reach the PSS (over-irradiated solutions). Thus, we repeated the experiment on multiple photoswitching by avoiding the irradiation until the PSSs. Remarkably, 15 photocycles were readily accomplished with **1** and **2** (Figure 13). Although small degree of photodegradation could be noticed in these experiments as well, the resistance to fatigue was significantly improved by irradiating under non-PSS conditions.

CONCLUSIONS

The unique iron(II) spin-crossover molecular switch **1** featuring a photochromic diarylethene-based ligand has been successfully modified. Methyl groups have been introduced into the phenanthroline-backbone of the photochrome (**2**), and phenyl groups have been introduced into the photoactive thiophenes (**3**). The photoswitchability of **2** and **3** has been investigated in solution at room temperature in detail and compared with that of **1** redone at similar conditions. While the modification of the phenanthroline unit had little influence on the photophysical properties of the molecular switch, the modification at the thiophenes decreased the thermal stability of the closed-ring isomer significantly. Multiple photoswitching has been readily achieved with **1** and **2** when the photostationary states were avoided. Further modifications of the phenanthroline backbone seem to be attractive for introducing anchoring groups thus targeting chemisorbed self-assembled monolayers.

ASSOCIATED CONTENT

Supporting Information

The Supporting Information is available free of charge on the ACS Publications website at DOI: 10.1021/acs.inorgchem.7b01952.

The details of computational, crystallographic, spectroscopic, and photophysical studies (PDF)

Accession Codes

CCDC 1560708−1560712 contain the supplementary crystallographic data for this paper. These data can be obtained free of charge via www.ccdc.cam.ac.uk/data_request/cif, or by emailing data_request@ccdc.cam.ac.uk, or by contacting The Cambridge Crystallographic Data Centre, 12 Union Road, Cambridge CB2 1EZ, UK; fax: +44 1223 336033.

AUTHOR INFORMATION

Corresponding Author

*E-mail: marat.khusniyarov@fau.de.

ORCID

Frank W. Heinemann: 0000-0002-9007-8404
Julien Bachmann: 0000-0001-6480-6212
Marat M. Khusniyarov: 0000-0002-2034-421X

Author Contributions

‡These authors contributed equally.

Notes

The authors declare no competing financial interest.

ACKNOWLEDGMENTS

This work was financially supported by the Fonds der Chemischen Industrie (Liebig Fellowship for M.M.K.), Deutsche Forschungsgemeinschaft (DFG Research Grant No. KH 279/3), and Emerging Talents Initiative (ETI) program of FAU Erlangen-Nürnberg. Prof. K. Meyer (FAU Erlangen-Nürnberg) is acknowledged for providing access to spectroscopic facilities and his general support. We thank Dr. J. Sutter for measuring Mössbauer spectra and Dr. A. Scheurer for the assistance with variable-temperature NMR spectroscopy.

REFERENCES

(1) Halcrow, M. A. *Spin-Crossover Materials, Properties and Applications;* John Wiley & Sons, Ltd., 2013.

DOI: 10.1021/acs.inorgchem.7b01952
Inorg. Chem. XXXX, XXX, XXX−XXX

(2) Gütlich, P.; Goodwin, H. A. *Spin Crossover in Transition Metal Compounds I-III, Topics in Current Chemistry;* Springer-Verlag: Berlin, Germany, 2004; Vol. *233*−*235*.
(3) Jureschi, C.-M.; Linares, J.; Boulmaali, A.; Dahoo, P.; Rotaru, A.; Garcia, Y. Pressure and Temperature Sensors Using Two Spin Crossover Materials. *Sensors* **2016**, *16* (2), 187.
(4) Quintero, C. M.; Félix, G.; Suleimanov, I.; Sanchez Costa, J.; Molnár, G.; Salmon, L.; Nicolazzi, W.; Bousseksou, A. Hybrid spin-crossover nanostructures. *Beilstein J. Nanotechnol.* **2014**, *5*, 2230−2239.
(5) Kahn, O.; Martinez, C. J. Spin-transition polymers: From molecular materials toward memory devices. *Science* **1998**, *279* (5347), 44−48.
(6) Létard, J.-F.; Guionneau, P.; Goux-Capes, L. Towards spin crossover applications. *Top. Curr. Chem.* **2004**, *235*, 221−249.
(7) Sanvito, S. Molecular spintronics. *Chem. Soc. Rev.* **2011**, *40* (6), 3336−3355.
(8) Ruiz, E. Charge transport properties of spin crossover systems. *Phys. Chem. Chem. Phys.* **2014**, *16* (1), 14−22.
(9) Bertoni, R.; Lorenc, M.; Cailleau, H.; Tissot, A.; Laisney, J.; Boillot, M.-L.; Stoleriu, L.; Stancu, A.; Enachescu, C.; Collet, E. Elastically driven cooperative response of a molecular material impacted by a laser pulse. *Nat. Mater.* **2016**, *15* (6), 606−610.
(10) Bairagi, K.; Iasco, O.; Bellec, A.; Kartsev, A.; Li, D.; Lagoute, J.; Chacon, C.; Girard, Y.; Rousset, S.; Miserque, F.; Dappe, Y. J.; Smogunov, A.; Barreteau, C.; Boillot, M.-L.; Mallah, T.; Repain, V. Molecular-scale dynamics of light-induced spin cross-over in a two-dimensional layer. *Nat. Commun.* **2016**, *7*, 12212.
(11) Lefter, C.; Rat, S.; Costa, J. S.; Manrique-Juárez, M. D.; Quintero, C. M.; Salmon, L.; Séguy, I.; Leichle, T.; Nicu, L.; Demont, P.; Rotaru, A.; Molnár, G.; Bousseksou, A. Current Switching Coupled to Molecular Spin-States in Large-Area Junctions. *Adv. Mater.* **2016**, *28* (34), 7508−7514.
(12) Bernien, M.; Naggert, H.; Arruda, L. M.; Kipgen, L.; Nickel, F.; Miguel, J.; Hermanns, C. F.; Krüger, A.; Krüger, D.; Schierle, E.; Weschke, E.; Tuczek, F.; Kuch, W. Highly Efficient Thermal and Light-Induced Spin-State Switching of an Fe(II) Complex in Direct Contact with a Solid Surface. *ACS Nano* **2015**, *9* (9), 8960−8966.
(13) Naggert, H.; Rudnik, J.; Kipgen, L.; Bernien, M.; Nickel, F.; Arruda, L. M.; Kuch, W.; Näther, C.; Tuczek, F. Vacuum-evaporable spin-crossover complexes: physicochemical properties in the crystalline bulk and in thin films deposited from the gas phase. *J. Mater. Chem. C* **2015**, *3* (30), 7870−7877.
(14) Warner, B.; Oberg, J. C.; Gill, T. G.; El Hallak, F.; Hirjibehedin, C. F.; Serri, M.; Heutz, S.; Arrio, M.-A.; Sainctavit, P.; Mannini, M.; Poneti, G.; Sessoli, R.; Rosa, P. Temperature- and Light-Induced Spin Crossover Observed by X-ray Spectroscopy on Isolated Fe(II) Complexes on Gold. *J. Phys. Chem. Lett.* **2013**, *4* (9), 1546−1552.
(15) Naggert, H.; Bannwarth, A.; Chemnitz, S.; von Hofe, T.; Quandt, E.; Tuczek, F. First observation of light-induced spin change in vacuum deposited thin films of iron spin crossover complexes. *Dalton Trans.* **2011**, *40* (24), 6364−6366.
(16) Gütlich, P.; Hauser, A.; Spiering, H. Thermal and Optical Switching of Iron(II) Complexes. *Angew. Chem., Int. Ed. Engl.* **1994**, *33* (20), 2024−2054.
(17) Létard, J.-F.; Guionneau, P.; Nguyen, O.; Costa, J. S.; Marcén, S.; Chastanet, G.; Marchivie, M.; Goux-Capes, L. A Guideline to the Design of Molecular-Based Materials with Long-Lived Photomagnetic Lifetimes. *Chem. - Eur. J.* **2005**, *11* (16), 4582−4589.
(18) McCusker, J. K.; Rheingold, A. L.; Hendrickson, D. N. Variable-Temperature Studies of Laser-Initiated $^5T_2$ –> $^1A_1$ Intersystem Crossing in Spin-Crossover Complexes: Empirical Correlations between Activation Parameters and Ligand Structure in a Series of Polypyridyl Ferrous Complexes. *Inorg. Chem.* **1996**, *35* (7), 2100−2112.
(19) Stock, P.; Pędziński, T.; Spintig, N.; Grohmann, A.; Hörner, G. High Intrinsic Barriers against Spin-State Relaxation in Iron(II)-Complex Solutions. *Chem. - Eur. J.* **2013**, *19* (3), 839−842.
(20) Khusniyarov, M. M. How to Switch Spin-Crossover Metal Complexes at Constant Room Temperature. *Chem. - Eur. J.* **2016**, *22* (43), 15178−15191.
(21) Witt, A.; Heinemann, F. W.; Sproules, S.; Khusniyarov, M. M. Modulation of Magnetic Properties at Room Temperature: Coordination-Induced Valence Tautomerism in a Cobalt Dioxolene Complex. *Chem. - Eur. J.* **2014**, *20* (35), 11149−11162.
(22) Witt, A.; Heinemann, F. W.; Khusniyarov, M. M. Bidirectional photoswitching of magnetic properties at room temperature: ligand-driven light-induced valence tautomerism. *Chem. Sci.* **2015**, *6* (8), 4599−4609.
(23) Milek, M.; Heinemann, F. W.; Khusniyarov, M. M. Spin Crossover Meets Diarylethenes: Efficient Photoswitching of Magnetic Properties in Solution at Room Temperature. *Inorg. Chem.* **2013**, *52* (19), 11585−11592.
(24) Rösner, B.; Milek, M.; Witt, A.; Gobaut, B.; Torelli, P.; Fink, R. H.; Khusniyarov, M. M. Reversible Photoswitching of a Spin-Crossover Molecular Complex in the Solid State at Room Temperature. *Angew. Chem., Int. Ed.* **2015**, *54* (44), 12976−12980.
(25) Boillot, M.-L.; Zarembowitch, J.; Sour, A. Ligand-Driven Light-Induced Spin Change (LD-LISC): A Promising Photomagnetic Effect. *Top. Curr. Chem.* **2004**, *234*, 261−276.
(26) Khusniyarov, M. M. Light-Induced Spin-Crossover. In *Reference Module in Chemistry, Molecular Sciences and Chemical Engineering;* Reedijk, J., Ed.; Elsevier, 2015.
(27) Roux, C.; Zarembowitch, J.; Gallois, B.; Granier, T.; Claude, R. Toward Ligand-Driven Light-Induced Spin Changing. Influence of the Configuration of 4-Styrylpyridine (stpy) on the Magnetic Properties of $Fe^{II}(stpy)_4(NCS)_2$ Complexes. Crystal Structures of the Spin-Crossover Species $Fe(trans\text{-}stpy)_4(NCS)_2$ and of the High-Spin Species $Fe(cis\text{-}stpy)_4(NCS)_2$. *Inorg. Chem.* **1994**, *33* (10), 2273−2279.
(28) Boillot, M.-L.; Chantraine, S.; Zarembowitch, J.; Lallemand, J. Y.; Prunet, J. First ligand-driven light-induced spin change at room temperature in a transition-metal molecular compound. *New J. Chem.* **1999**, *23* (2), 179−183.
(29) Hasegawa, Y.; Kume, S.; Nishihara, H. Reversible light-induced magnetization change in an azobenzene-attached pyridylbenzimidazole complex of iron(II) at room temperature. *Dalton Trans.* **2009**, *2*, 280−284.
(30) Hasegawa, Y.; Takahashi, K.; Kume, S.; Nishihara, H. Complete solid state photoisomerization of bis(dipyrazolylstyrylpyridine)iron(II) to change magnetic properties. *Chem. Commun.* **2011**, *47* (24), 6846−6848.
(31) Takahashi, K.; Hasegawa, Y.; Sakamoto, R.; Nishikawa, M.; Kume, S.; Nishibori, E.; Nishihara, H. Solid-State Ligand-Driven Light-Induced Spin Change at Ambient Temperatures in Bis(dipyrazolylstyrylpyridine)iron(II) Complexes. *Inorg. Chem.* **2012**, *51* (9), 5188−5198.
(32) Venkataramani, S.; Jana, U.; Dommaschk, M.; Sönnichsen, F. D.; Tuczek, F.; Herges, R. Magnetic Bistability of Molecules in Homogeneous Solution at Room Temperature. *Science* **2011**, *331* (6016), 445−448.
(33) Feringa, B. L.; Browne, W. R. *Molecular Switches;* Wiley-VCH Verlag: Weinheim, Germany, 2011; Vol. *1*−*2*.
(34) Thiele, S.; Malmgaard-Clausen, M.; Engel-Andreasen, J.; Steen, A.; Rummel, P. C.; Nielsen, M. C.; Gloriam, D. E.; Frimurer, T. M.; Ulven, T.; Rosenkilde, M. M. Modulation in Selectivity and Allosteric Properties of Small-Molecule Ligands for CC-Chemokine Receptors. *J. Med. Chem.* **2012**, *55* (18), 8164−8177.
(35) Ko, C.-C.; Kwok, W.-M.; Yam, V. W.-W.; Phillips, D. L. Triplet MLCT photosensitization of the ring-closing reaction of diarylethenes by design and synthesis of a photochromic rhenium(I) complex of a diarylethene-containing 1,10-phenanthroline ligand. *Chem. - Eur. J.* **2006**, *12* (22), 5840−5848.
(36) Lim, S.-J.; An, B.-K.; Park, S. Y. Bistable Photoswitching in the Film of Fluorescent Photochromic Polymer: Enhanced Fluorescence Emission and Its High Contrast Switching. *Macromolecules* **2005**, *38* (15), 6236−6239.

DOI: 10.1021/acs.inorgchem.7b01952
Inorg. Chem. XXXX, XXX, XXX−XXX

(37) Hill, A. F.; Malget, J. M.; White, A. J. P.; Williams, D. J. Dihydrobis(pyrazolyl)borate Alkylidyne Complexes of Tungsten. *Eur. J. Inorg. Chem.* **2004**, *2004*, 818−828.
(38) Kühni, J.; Adamo, V.; Belser, P. Synthesis of an unsymmetrically substituted, dithienylethene-containing 1,10-phenanthroline ligand and its ruthenium(II) complex. *Synthesis* **2006**, *2006*, 1946−1948.
(39) Walton, I. M.; Cox, J. M.; Benson, C. A.; Patel, D. G.; Chen, Y.-S.; Benedict, J. B. The role of atropisomers on the photo-reactivity and fatigue of diarylethene-based metal-organic frameworks. *New J. Chem.* **2016**, *40* (1), 101−106.
(40) Chesneau, B.; Passelande, A.; Hudhomme, P. Efficient Access to a Versatile 5,6-Dithio-1,10-phenanthroline Building Block and Corresponding Organometallic Complexes. *Org. Lett.* **2009**, *11* (3), 649−652.
(41) Bill, E. *MFIT,* version 1.1; MPI for Bioinorganic Chemistry: Mülheim/Ruhr, Germany, 2008.
(42) *SADABS,* 2008/1; Bruker AXS, Inc.: Madison, WI, 2009.
(43) Sheldrick, G. M. A short history of SHELX. *Acta Crystallogr., Sect. A: Found. Crystallogr.* **2008**, *64*, 112−122.
(44) Irie, M.; Fukaminato, T.; Matsuda, K.; Kobatake, S. Photochromism of Diarylethene Molecules and Crystals: Memories, Switches, and Actuators. *Chem. Rev.* **2014**, *114* (24), 12174−12277.
(45) Yam, V. W.-W.; Ko, C.-C.; Zhu, N. Photochromic and Luminescence Switching Properties of a Versatile Diarylethene-Containing 1,10-Phenanthroline Ligand and Its Rhenium(I) Complex. *J. Am. Chem. Soc.* **2004**, *126* (40), 12734−12735.
(46) Fukumoto, S.; Nakashima, T.; Kawai, T. Photon-Quantitative Reaction of a Dithiazolylarylene in Solution. *Angew. Chem., Int. Ed.* **2011**, *50* (7), 1565−1568.
(47) Li, W.; Jiao, C.; Li, X.; Xie, Y.; Nakatani, K.; Tian, H.; Zhu, W. Separation of Photoactive Conformers Based on Hindered Diarylethenes: Efficient Modulation in Photocyclization Quantum Yields. *Angew. Chem., Int. Ed.* **2014**, *53* (18), 4603−4607.
(48) Thompson, A. L.; Goeta, A. E.; Real, J. A.; Galet, A.; Carmen Muñoz, M. Thermal and light induced polymorphism in iron(II) spin crossover compounds. *Chem. Commun.* **2004**, *12*, 1390−1391.
(49) Kulmaczewski, R.; Shepherd, H. J.; Cespedes, O.; Halcrow, M. A. A Homologous Series of $[Fe(H_2Bpz_2)_2(L)]$ Spin-Crossover Complexes with Annelated Bipyridyl Co-Ligands. *Inorg. Chem.* **2014**, *53* (18), 9809−9817.
(50) Nihei, M.; Suzuki, Y.; Kimura, N.; Kera, Y.; Oshio, H. Bidirectional Photomagnetic Conversions in a Spin-Crossover Complex with a Diarylethene Moiety. *Chem. - Eur. J.* **2013**, *19* (22), 6946−6949.
(51) Real, J. A.; Muñoz, M. C.; Faus, J.; Solans, X. Spin Crossover in Novel Dihydrobis(1-pyrazolyl)borate $[H_2B(pz)_2]$-Containing Iron(II) Complexes. Synthesis, X-ray Structure, and Magnetic Properties of $[FeL\{H_2B(pz)_2\}_2]$ (L = 1,10-Phenanthroline and 2,2′-Bipyridine). *Inorg. Chem.* **1997**, *36* (14), 3008−3013.
(52) Gütlich, P.; Goodwin, H. A. Spin Crossover - An Overall Perspective. *Top. Curr. Chem.* **2004**, *233*, 1−47.
(53) Note that magnetic measurements on 1 were always performed on powder samples obtained from MeOH solutions. This was not explicitly mentioned in our previous works.
(54) Irie, M. Diarylethenes for Memories and Switches. *Chem. Rev.* **2000**, *100* (5), 1685−1716.
(55) Gilat, S. L.; Kawai, S. H.; Lehn, J.-M. Light-Triggered Molecular Devices: Photochemical Switching Of optical and Electrochemical Properties in Molecular Wire Type Diarylethene Species. *Chem. - Eur. J.* **1995**, *1* (5), 275−284.
(56) Patel, P. D.; Masunov, A. E. Theoretical Study of Photochromic Compounds: Part 3. Prediction of Thermal Stability. *J. Phys. Chem. C* **2011**, *115* (20), 10292−10297.

DOI: 10.1021/acs.inorgchem.7b01952
Inorg. Chem. XXXX, XXX, XXX−XXX